Journal of Solid Mechanics Vol. 9, No. 3 (2017) pp. 599-607

# A New Approach to Buckling Analysis of Lattice Composite Structures

S.A. Galehdari [1, 2 *], A.H. Hashemian [3], J.E. Jam [4], A. Atrian [1, 2]

[1] *Department of Mechanical Engineering, Najafabad Branch ,Islamic Azad University, Najafabad, Iran*
[2] *Modern Manufacturing Technologies Research Center, Najafabad Branch ,Islamic Azad University, Najafabad, Iran*
[3] *Mechanical and Aerospace Engineering Department, Science and Research Branch, Islamic Azad University ,Tehran, Iran*
[4] *Composite Material & Technology, Malek Ashtar University of Technology, Tehran, Iran*

Received 26 June 2017; accepted 22 August 2017

**ABSTRACT**

Buckling strength of composite latticed cylindrical shells is one of the important parameters for studying the failure of these structures. In this paper, new governing differential equations are derived for latticed cylindrical shells and their critical buckling axial loads. The nested structure under compressive axial buckling load was analyzed. Finite Element Method (FEM) was applied to model the structure in order to verify the analytical results. The obtained results were validated based upon the results of previous case studies in literature. For the squared type of lattice composite shells, a new formula for the buckling load was developed and its value was compared to the critical load, using FEM with 3D beam elements. The processes were carried out for three different materials of Carbon/Epoxy, Kevlar/Epoxy and EGlass/Epoxy.


**Keywords:** Lattice structures; Composite materials; Finite element method; Buckling loading.

## 1 INTRODUCTION

NOWADAYS, many researchers have both theoretically and experimentally investigated buckling strength of composite cylindrical shells. In 1981 Rehfield et al. made an intensive study on the buckling strength of composite isogrid cylindrical shells and wide columns [1]. They found that local crippling of the ribs and skins buckling differ substantially from general buckling in terms of practical consequences for compressed stiffened cylindrical shells. Hosomura et al. [2] investigated the failure of cylindrical grid using finite element method and experimental tests. In this work, three dimensional straight beam elements were used. Also many other researchers (Hayashi [3], Kobayashi [4], Simitses [5] and Onoda [6]) investigated the buckling strength of composite cylindrical shells theoretically and experimentally. Chin et al [7] have studied the buckling behavior of composite hull structures for underwater service and suggested a design procedure for the most weight efficient structure with the highest buckling load using finite element method. Philips et al. [8] have discussed a smearing method for determining the global buckling load of this type of stiffened panel. Later on Graham [9] presented an analytical method for determining the buckling loads of ring and stringer stiffened cylinders. Also Pshenichnov et al. [10] preformed a new decomposition method for solving boundary value problems on the bending of latticed plates of various types with the general boundary conditions on the contour. By this method the problem is reduced to a one-dimensional integral equation, which can be solved by the grid method. Holzer et al. [11] have determined the

*Corresponding author. Tel.: +98 9399238836; Fax: +98 31 42292537.
*E-mail address: ali.galehdari@pmc.iaun.ac.ir* (A.Galehdari).

governing failure mode and the ultimate snow loads of a wood dome using finite element method. The dome consisted of a triangulated network of curved wood beams. Each beam of the dome has been modelled by two straight, three dimensional, Bernoulli/Euler beam elements. Holzer found that the large curvature and slenderness of the beams made it unnecessary to use curved beam elements or to include shear deformation. Vassiliev et al. [12-13] made a complete research about designing and manufacturing of lattice structures by filament winding and wet winding methods. Totaro et al. [14] conducted some experiments on the subject of filament wound composite anisogrid structures. The main phases of design, manufacturing and testing are explored giving a rather comprehensive methodology to address the kind of concept toward primary structures for aerospace application aiming at structural efficiency and process reliability. Fan et al. [15] developed new techniques to make materials with a periodic three-dimensional lattice structure. Epoxy-Soaked continuous carbon fibers were first introduced to make lattice composite structure with maximum specific stiffness. An intertwining method was chosen and developed as the best route to make lattice composite materials reinforced by carbon fibers.

Akbari Alashti et al. [16] have studied the buckling behavior of a composite lattice cylindrical shell and effects of rib defects on the distribution of stress field. In this research a finite element buckling analysis of the structure has been carried out by ANSYS software. Ghorbanpour Arani et al. [17] have investigated the buckling and postbuckling behaviors of a composite beam with single delamination using the commercial code ANSYS. In this research, effect of delamination length, position through thickness and stacking sequence of the plies on the buckling and postbuckling of laminates have been studied. It has been found that significant decreases occur in the critical buckling loads after a certain value of the delamination length. Eskandari Jam et al. [18] have studied the buckling analysis of circular annular plate reinforced by carbon nanotubes (CNTs) subjected to compressive and torsional loads with various axially symmetric boundary conditions. In this paper, the eigenvalues of the problem are obtained by means of an analytical approach based on the optimized Rayleigh-Ritz method. The effects of CNTs orientation angles, edge conditions, geometric ratio of plate and agglomeration of the randomly oriented straight CNTs have been investigated on the critical buckling loads.

In this paper, the general buckling equation of a latticed composite shell was derived. Subsequently, a general relation for the buckling load was obtained for the special case of squared, latticed composite shell. Finally, the results were validated using FE method.

## 2 MATHEMATICAL FORMULATION OF LATTICE STRUCTURE THEORIES

In Fig.1, local curvilinear system of the orthogonal coordinates $\alpha, \beta$ and the normal to the surface is shown.

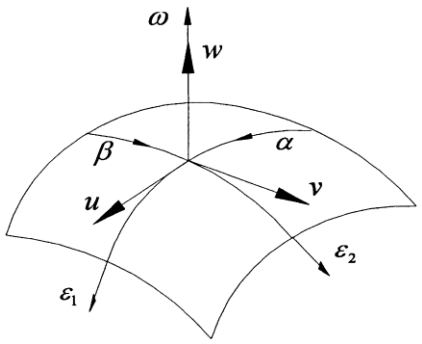


**Fig.1**
Median surface of a shell curvilinear coordinates.

Based upon the thin-walled shell theory, the strains and curvature changes of the shell's middle surface can be determined using the components of the displacement vector *u,v* and *w* [19]:

$$\varepsilon_1 = \frac{1}{R}\frac{\partial u}{\partial \alpha} \qquad \varepsilon_2 = \frac{1}{R}\left(\frac{\partial v}{\partial \beta} + w\right) \qquad \gamma_{12} = \frac{1}{R}\left(\frac{\partial u}{\partial \beta} + \frac{\partial v}{\partial \alpha}\right) \tag{1}$$

$$k_1 = -\frac{1}{R^2}\frac{\partial^2 w}{\partial \alpha^2} \qquad k_2 = -\frac{1}{R^2}\frac{\partial^2 w}{\partial \beta^2} \qquad \tau = -\frac{1}{R^2}\frac{\partial^2 w}{\partial \alpha \partial \beta} \tag{2}$$

The quantities of $\varepsilon_1, \varepsilon_2$ and $\gamma_{12}$ refer to the normal and shear strains of the point in the middle surface, respectively. $k_1$ and $k_2$ represent changes in the curvature of the middle surface during deformation. Moreover, the amount of $\tau$ indicates the twisting of the middle surface during deformation. Fig. 2 demonstrates a lattice with four families of members. The parameter $a_i$ is defined as a member length of the $i^{th}$ member and the parameter $\varphi_i$ is defined as the angle between axis $\alpha$ and the member's axis.

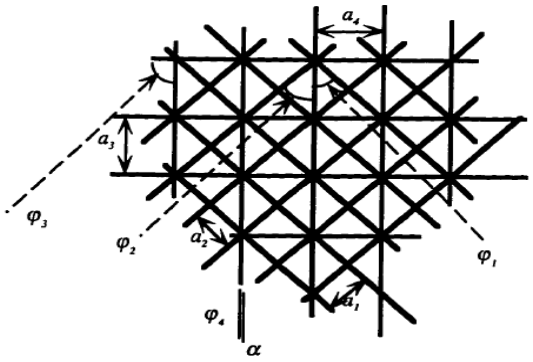


**Fig.2**
Lattice with four families of members.

As two members have crossed at a point, it is assumed that they have equal lengths *i.e.*, $a_1 = a_2 = a$ and $\varphi_1 = -\varphi_2 = \varphi$. Strains and curvature changes of a point on the middle surface of the $i^{th}$ member in the deformed state in terms of $\varepsilon_1, \varepsilon_2, \gamma_{12}, k_1, k_2$ and $\tau$ are:

$$\varepsilon^*_i = \varepsilon_1 c_i^2 + \varepsilon_2 s_i^2 + \gamma_{12} s_i c_i \qquad k^*_i = k_1 c_i^2 + k_2 s_i^2 + k \sin(2\varphi)_i \qquad \tau^*_i = (k_2 - k_1) c_i s_i + \tau \cos(2\varphi)_i \tag{3}$$

where: $c_i = \cos\varphi_i, s_i = \sin\varphi_i$

The quantities of $\varepsilon_i^*, k_i^*$ and $\tau_i^*$ represent the normal strain in the longitudinal direction. The curvature change due to the bending moment is represented by $M_i^*$, and the twisting angle of the $i^{th}$ member due to the twisting moment is given by $H_i^*$.

$$N_i^* = E_i A_i \varepsilon_i^* \qquad Q_i^* = -\nabla_i M_i^* \qquad S_i^* = -\nabla_i G_i^* \tag{4}$$

The system of moments is:

$$M_i^* = -E_i J_{1i} k_i^* \qquad G_i^* = -E_i J_{2i} k_i^0 \qquad H_i^* = -G_i J_{3i} \tau_i^* \tag{5}$$

The change of the rod's axis of curvature in the plane tangent to the shell's middle surface can be derived using the formula [20]:

$$\begin{cases} k_i^0 = -\nabla_i \Psi_i \\ 2\Psi_i = -2\delta_i + \gamma_{12}\cos(2\varphi)_i + (\varepsilon_2 - \varepsilon_1)\sin(2\varphi)_i \end{cases} \tag{6}$$

In which; $\nabla_i = \left( \frac{c_i}{A^*}\frac{\partial}{\partial\alpha} + \frac{s_i}{B^*}\frac{\partial}{\partial\beta} \right)$ where $A^*$ and $B^*$ are coefficients of the first quadratic form of the shell's middle surface, and $E_i$ and $G_i$ are Young's modulus and shear modulus of the $i^{th}$ member respectively. In addition, $A_i, J_{1i}, J_{2i}, J_{3i}$ are respectively the member's cross-sectional area, bending sectional moment with respect to *x*-axis, bending sectional moment with respect to *y*-axis, and twisting sectional moment. Moreover, $k_i^0 = -\nabla_i \Psi$ and $\Psi$ is the turning angle of the fiber projection defined as, $2\Psi_i = -2\delta_i + \gamma_{12}\cos(2\varphi)_i + (\varepsilon_2 - \varepsilon_1)\sin(2\varphi)_i$ in which

$\delta_i = \frac{E_i A_i}{E_1 A_1}$. In the aforementioned equation, $A_i$ is the cross-section area and $E_i$ is the Young's modulus of the $i^{th}$ member [20]. Fig. 3 demonstrates the system of forces ($N_i^*, Q_i^*, S_i^*$) and ($M_i^*, G_i^*, H_i^*$) in the cross-section of the $i^{th}$ member.

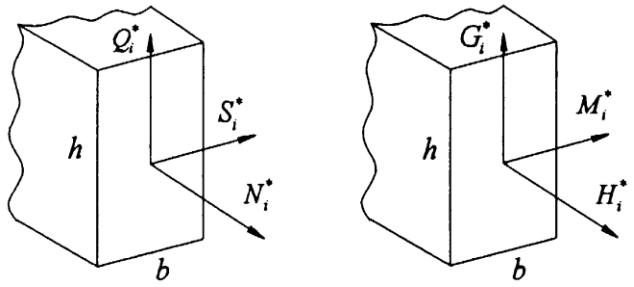


**Fig.3**
Positive directions of forces and moments in the cross-section of the ribs.

The relations between the system of internal forces, the moments with external system of forces and moments in a shell element are as follows (see Figure 4) [21]:

$$N_1 = \sum_{i=1}^{n} (N_i^* c_i^2 - S_i^* s_i c_i)/a_i \qquad N_2 = \sum_{i=1}^{n} (N_i^* s_i^2 + S_i^* s_i c_i)/a_i$$
$$S_1 = \sum_{i=1}^{n} (N_i^* s_i c_i + S_i^* c_i^2)/a_i \qquad S_2 = \sum_{i=1}^{n} (N_i^* s_i c_i - S_i^* s_i^2)/a_i \tag{7}$$
$$Q_1 = \sum_{i=1}^{n} \frac{Q_i^* c_i}{a_i} \qquad Q_2 = \sum_{i=1}^{n} \frac{Q_i^* s_i}{a_i}$$

$$M_1 = \sum_{i=1}^{n} (M_i^* c_i^2 + H_i^* s_i c_i)/a_i \qquad M_2 = \sum_{i=1}^{n} (M_i^* s_i^2 - H_i^* s_i c_i)/a_i$$
$$H_1 = -\sum_{i=1}^{n} (M_i^* s_i c_i - H_i^* c_i)/a_i \qquad H_2 = -\sum_{i=1}^{n} (M_i^* s_i c_i + H_i^* s_i)/a_i \tag{8}$$
$$M_{1s} = \sum_{i=1}^{n} \frac{G_i^* c_i}{a_i} \qquad M_{2s} = -\sum_{i=1}^{n} \frac{G_i^* s_i}{a_i}$$

where $n$ defines the class of grid configuration e.g. for a triangle lattice; $n=3$ and for a square lattice, $n=2$. $N_1, S_1, N_2, S_2$ are respectively in-plane internal normal and shear forces; $Q_1, Q_2$ are internal transverse shear forces; $M_1, M_{s1}, M_2, M_{s2}$ are internal bending moments, and $H_1, H_2$ are internal twisting moments, all per unit of length.

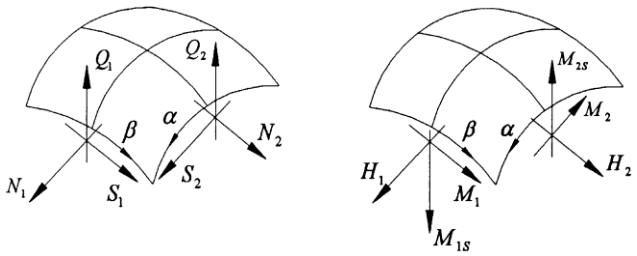


**Fig.4**
Direction of forces and moments acting in the shell.

The equilibrium equations for the cylindrical shell's element while neglecting body forces are:

$$\frac{1}{R}\left(\frac{\partial N_1}{\partial \alpha}+\frac{\partial S_1}{\partial \beta}\right)+X=0 \qquad \frac{1}{R}\left(\frac{\partial N_2}{\partial \beta}+\frac{\partial S_2}{\partial \alpha}\right)+Y=0 \qquad \frac{1}{R}\left(\frac{\partial Q_1}{\partial \alpha}+\frac{\partial Q_2}{\partial \beta}-N_2\right)+Z=0 \tag{9}$$

where *X, Y* and *Z* are the external forces and *R* is the lattice shell's radius. Summation of moments in the $\alpha$ and $\beta$ directions are given by:

$$Q_1=\frac{1}{R}\left(\frac{\partial H_2}{\partial \beta}-\frac{\partial M_1}{\partial \alpha}\right) \qquad Q_2=\frac{1}{R}\left(\frac{\partial H_1}{\partial \alpha}-\frac{\partial M_2}{\partial \beta}\right) \tag{10}$$

By combining Eqs. (1) to (9) and expressing forces and moments in terms of displacement components [22], Eq. (11) can be obtained as mentioned below:

$$L_{11}(u)+L_{12}(v)+L_{13}(w)=-R^2X \qquad L_{21}(u)+L_{22}(v)+L_{23}(w)=-R^2Y \qquad L_{31}(u)+L_{32}(v)+L_{33}(w)=R^2Z \tag{11}$$

## 3 BUCKLING OF SQUARED LATTICED SHELL

For a cylindrical square cell, the angles are $\varphi_1=-\varphi_2=45^{\circ}$ and $J_3=0$. By substituting $n=2$ in Eqs. (7) and (8), and setting external forces equal to zero, the forces $N_1$, $N_2$ and $S_2$ will be obtained as follows

$$\begin{aligned} &N_1=2K\cos^2(\varphi)\left(\cos^2(\varphi)\varepsilon_1+\sin^2(\varphi)\varepsilon_2\right) \qquad N_2=2K\cos^2(\varphi)\left(\cos^2(\varphi)\varepsilon_1+\sin^2(\varphi)\varepsilon_2\right)\cot^2(\varphi) \\ &S_1=S_2=2K\sin^2(\varphi)\cos^2(\varphi)w \end{aligned} \tag{12}$$

By inserting values of $\varphi_1$, $\varphi_2$, $N_1, N_2$, $S_1$ and $S_2$ in general forms of *L* operators; assuming $X=Y=0$, and respecting the fact that in this case, $\xi=\alpha, u^*=u$, Eq. (11) can be simplified to:

$$\begin{aligned} &\frac{\partial^2 u}{\partial \xi^2}+\frac{\partial^2 u}{\partial \beta^2}+2\frac{\partial^2 v}{\partial \xi \partial \beta}+\frac{\partial w}{\partial \xi}=0 \\ &2\frac{\partial^2 u}{\partial \xi \partial \beta}+\frac{\partial^2 v}{\partial \xi^2}+\frac{\partial^2 v}{\partial \beta^2}+\frac{\partial w}{\partial \beta}=0 \\ &\frac{\partial u}{\partial \xi}+\frac{\partial v}{\partial \beta}+\left(\frac{\partial^4 w}{\partial \xi^4}+6\frac{\partial^4 w}{\partial \xi^2 \partial \beta^2}+\frac{\partial^4 w}{\partial \beta^4}\right)r_1^2-w-\frac{2R^2}{K}Z_1=0 \end{aligned} \tag{13}$$

Of note is that in the above-mentioned relation, $Z_1=Z/4\sin^4_{\varphi}$. By using Eq. (13) and the exact form of $\Phi$ function, the particular solution for the system of external loads can be derived as follows:

$$u=\frac{\partial}{\partial \xi}\left(\frac{\partial^2}{\partial \beta^2}-\frac{\partial^2}{\partial \xi^2}\right)\Phi \qquad v=\frac{\partial}{\partial \xi}\left(\frac{\partial^2}{\partial \xi^2}-\frac{\partial^2}{\partial \beta^2}\right)\Phi \qquad w=\left(\frac{\partial^4}{\partial \xi^4}+6\frac{\partial^4}{\partial^2 \xi \partial^2 \beta}+\frac{\partial^4}{\partial \beta^4}\right)\Phi \tag{14}$$

It can be assumed that the appropriate form of $\Phi$ function for the current case is:

$$\Phi(\xi,\beta)=\sum_{k=0}^{\infty} f_k(\xi)\cos(k\beta) \tag{15}$$

where $f_k(\xi)$ is a function that should be defined.

In the axial buckling analysis, it is clear that $X = Y = 0$ and $Z \neq 0$ (compressive). In order to carry out the buckling study, Eq. (15) was substituted for Eq. (13), and by setting $X = Y = 0$ and $Z$ values, the following relation for $f_k(\xi)$ was derived:

$$\left(1+\gamma\tan_{\varphi}^{2}\right)\frac{\partial^4 f_k}{\partial\xi^4}-\left[\,6k^2+2k^2\gamma\left(\frac{2}{\sin_{2\varphi}^{2}}-3\right)-q\,\right]\frac{\partial^2 f_k}{\partial\xi^2}+k^2\left[\,(1+\gamma\cot_{\varphi}^{2})k^2-q\,\right]f_k=0 \tag{16}$$

Eq. (16) can be met in case $f_k(\xi)$ is considered as:

$$f_k(\xi)=\sum_{m=1}^{\infty}A_{km}\sin(\lambda_m\xi) \tag{17}$$

where, $l_m = mp/x_0, \xi_0$ is the initial length of the cylinder and $A_{km}$ are constant coefficients which can be found by applying boundary conditions.

By back-substitution of $f_k(\xi)$ into Eq. (15), the following form for $\Phi$ function will be obtained:

$$\Phi(\xi,\beta)=\sum_{k=0}^{\infty}\sum_{m=1}^{\infty}A_{km}\sin(\lambda_m\xi)\cos(k\beta) \tag{18}$$

Substituting Eq. (18) in Eqs. (14), *u, v* and *w* would be:

$$\begin{aligned}
u &= \sum_{k=0}^{\infty}\sum_{m=1}^{\infty}A_{km}\left(\left(\lambda_m^2-k^2\right)\lambda_m\right)\cos(\lambda_m\xi)\cos(k\beta)\\
v &= \sum_{k=0}^{\infty}\sum_{m=1}^{\infty}A_{km}\left(\left(k^2-\lambda_m^2\right)\lambda_m\right)\cos(\lambda_m\xi)\cos(k\beta)\\
w &= \sum_{k=0}^{\infty}\sum_{m=1}^{\infty}A_{km}\left(\lambda_m^4-2\lambda_m^2k^2+k^4\right)\sin(\lambda_m\xi)\cos(k\beta)
\end{aligned} \tag{19}$$

From Eq. (12), for a square lattice cell where $\varphi = 90^{o}$, it can be clear that $N_2 = 0$. Having the values for *u, v* and *w,* strain components can be derived using Eqs. (1)-(2). Thereafter, by substituting the derived strains in Eq. (4), the values for $N^*$ can be calculated, and by implementing Eq. (7) we will have:

$$N=\frac{2EA}{Ra}\sin_{\varphi}^{2}\sum_{k=0}^{\infty}\sum_{m=1}^{\infty}A_{km}\left\{\begin{bmatrix}k^2\lambda_m^2\cos_{\varphi}^{2}-\lambda_m^4\cos_{\varphi}^{2}\\+\left(\lambda_m^4-2k^2\lambda_m^2+k^4\right)\end{bmatrix}\sin(\lambda_m\xi)\cos(k\beta)+\left(\lambda_m^3-\lambda_mk^3\right)\cos(\lambda_m\xi)\sin(k\beta)\right\} \tag{20}$$

The critical value for *N* occurs when $k = 0$ and $m = 1$, which means:

$$(N)_{cr}=\frac{2EA}{Ra}A_{01}\sin_{\varphi}^{4}\left(\frac{\pi}{\xi_0}\right)^4\sin\left(\frac{\pi}{\xi_0}\xi\right) \tag{21}$$

where $A_{01}$ is a constant coefficient which can be calculated by applying boundary conditions as mentioned above.

## 4 RESULTS AND VERIFICATIONS

A new approach for the critical load of a squared lattice shell has been derived as represented in Eq. (21). Also finite element models have been considered for verifying the suitability and the accuracy of the analytical results. The FE model was simulated using commercially available software programs [23] in which a 3D beam element was used instead of each rib. It is noteworthy that the beam element used for this model was a uniaxial element with tension, compression, torsion and bending capabilities. The element has six degrees of freedom at each node, including translations in the nodal *x*, *y*, and *z* directions and rotations about the nodal *x*, *y* and *z* axes. Stress stiffening and large deflection capabilities were included as well. A consistent tangent stiffness matrix option is available for large deformation analyses. In order to obtain the numerical results, Carbon/Epoxy material was used, the mechanical properties of which are given in Table 1. The error between the analytical and the FEM results is given by:

$$\%Error = \frac{\left(N_{Analytical} - N_{FEM}\right)}{N_{Analytical}} \times 100 \tag{22}$$

**Table 1**
Properties of Selected Materials [24].

| Material Type | Mechanical Properties | | Geometric Properties | | | |
|---|---|---|---|---|---|---|
| | $E_1(GPa)$ | $\upsilon$ | $A_{01}$ | $\xi(m)$ | $\xi_0(m)$ | Radius$(m)$ |
| Carbon/Epoxy | 207 | 0.25 | | | | |
| Kevlar/Epoxy | 76 | 0.34 | $10^{-5}$ | 1.5 | $\xi/2$ | 1 |
| EGlass/Epoxy | 54 | 0.25 | | | | |

The maximum error between the analytical and FEM results (Eq. (22)) is about 7%. To the best of our knowledge at this stage, the achieved analytical results are of acceptable accuracy and for all applications. Moreover, the same calculations were performed for two other media, namely Kevlar/Epoxy and E-Glass/Epoxy with the same geometry and boundary conditions mentioned for the case study of Carbon/Epoxy material. The results for the first three critical buckling loads of the abovementioned composites were calculated using analytical and FE methods. These results along with the corresponding errors are listed in Table 2. The maximum error is approximately 7% for the first mode of Carbon/Epoxy material, and due to the convergence of the solutions in analytical method, the error reduces with the increase of the mode number. Under aforementioned conditions, squared lattice cylinders with longitudinal and circumferential ribs are efficient with external axial compressive forces. Based on Eq. (21), the values of critical buckling loads for the aforementioned materials are calculated and represented in Fig. 5. Furthermore, among all the materials which were used for modelling the squared latticed cylindrical shell, Carbon/Epoxy had the highest strength against external axial compressive forces. In other words, for square latticed cylindrical shells, materials with higher longitudinal modulus $(E_1)$ are more effective in handling axial compressive loads.

**Table 2**
Critical Buckling Modes of Lattice cylindrical shell.

| Material Type | Buckling Mode | Critical Buckling Load ($N$) | | Error (%) |
|---|---|---|---|---|
| | | Analytical | FEM | |
| Carbon/Epoxy | First | 14076 | 13080 | 7.07 |
| | Second | 13561 | 12580 | 7.23 |
| | Third | 13429 | 12420 | 7.51 |
| E-Glass/Epoxy | First | 3672 | 3412.8 | 7.05 |
| | Second | 3408.7 | 3412.8 | 0.12 |
| | Third | 3395.5 | 3369.6 | 0.76 |
| Kevlar/Epoxy | First | 5168 | 5411.2 | 4.49 |
| | Second | 5032 | 5411.2 | 7.53 |
| | Third | 4941 | 4924.8 | 0.32 |

## 5 CONCLUSIONS

A composite latticed cylindrical shell with square cells was analyzed and the governing equations were derived. The equations were followed to give the relation of critical buckling loads with respect to critical axial loads. The results for the critical buckling load using analytical method were compared with corresponding results from FEM analysis, indicating a well agreement in between. The following statements can be briefly noted as the results and conclusions accomplished through this study.

- Three critical buckling modes for three different materials are obtained using analytical and FE methods.
- Carbon/Epoxy has superior strength against axial external force; hence in designing squared latticed cells cylinders, this composite material has a pronounced merit over the other two.
- Composite materials with higher longitudinal modulus ( $E_1$ ) are more effective in designing the squared latticed cylindrical shells.

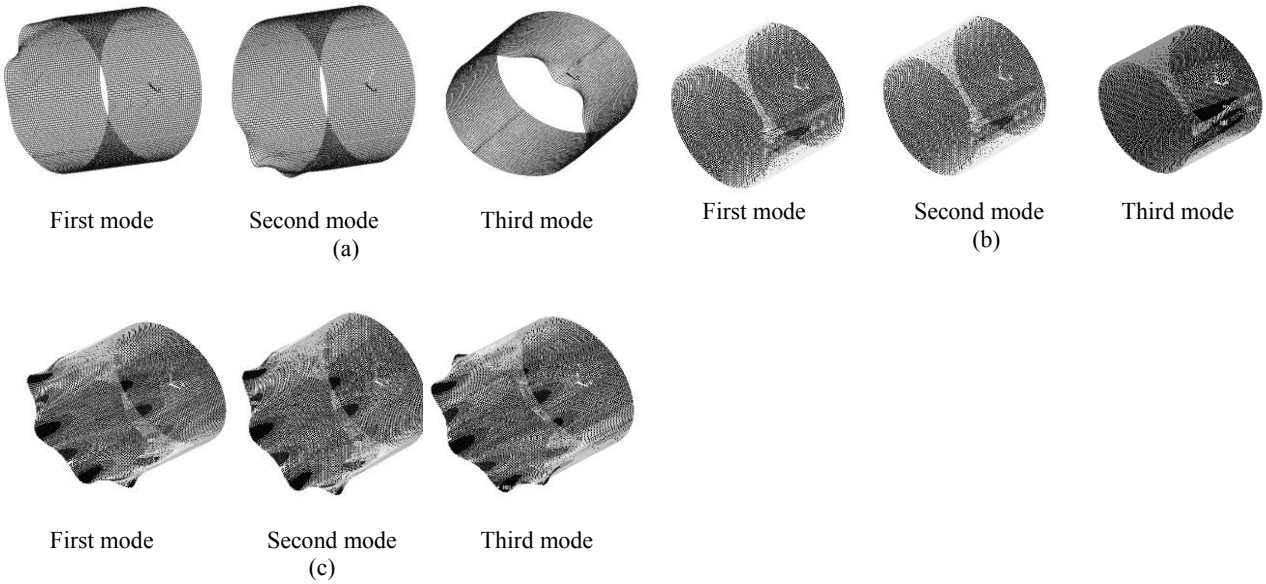


**Fig.5**
Deformation modes under critical load for: a) Carbon epoxy, b) Kevlar epoxy, c)E-glass epoxy.

## REFERENCES

[1] Rehfield L.W., Deo R.B., Renieri G., 1980, Continuous filament advanced composite isogrid: A promising structural concept, *Fibrous Composites in Structural Design* **1980**: 215-239.
[2] Hosmura T., Kawashima T., Mori D., 1981, New CFRP structural element, *Japan-US Conferences on Composite Materials*, Tokyo.
[3] Hayashi T., 1981, Buckling strength of cylindrical geodesic structures, *Japan-US conference on Composite Materials*, Tokyo.
[4] Kobayashi S., 1982, Compressive buckling of graphite-epoxy composite circular cylindrical shell, *Progress in Science and Engineering of Composites*, Tokyo.
[5] Simitses G. J., 1984, *An Introduction to the Elastic Stability of Structures*, Robert E. Krieger Publishing Company.
[6] Onoda J., 1985, Optimal laminate configurations of cylindrical shell for axial buckling, *AIAA Journal* **23**(7):1093-1098.
[7] Chin H. B., Prevorsek D. C., 1988, Design of composite hull structures for underwater service, *Proceeding of the Fourth Japan-U.S Conference on Composite Material*.
[8] Philips J.L., Gurdal Z., 1990, Structural analysis and optimum design of geodesically stiffened composite panels, *NASA Report CCMS-90-05*.
[9] Graham J., 1993, Preliminary techniques for ring and stinger stiffened cylindrical shells, *NASA report TM-108399*.

[10] Pshenichnov G.I., Klabukova L. S., Ul'yanova V. I., 1998, Solving boundary value problems concerning the bending of latticed rectangular plates by the decomposition method, *Journal of Computational Mathematics and Mathematical Physics* **38**(3): 419-434.
[11] Holzer S. M., Kavi S. A., Tongtoe S., Dolan J.D., 1994, What controls the ultimate load of a glulam dome, *Proceedings of the IASS Symposium'94*, Atlanta.
[12] Vasiliev V.V., Barynin V. A., Rasin A.F., 2001, Anisogrid lattice structures- survey of development and application, *Journal of Composite Structures* **54**: 361-370.
[13] Vasiliev V.V., Rasin A.F. ,2006, Anisogrid composite lattice structures for spacecraft and aircraft applications, *Journal of Composite Structures* **76**:182-189.
[14] Totaro G., De Nicola F., 2005, Optimization and manufacturing of composite cylindrical anisogrid structures, *AIAA/CIRA 13th International Space Planes and Hypersonics Systems and Technologies*, *Centro Italiano Ricerche Aerospaziali*, Capua, Italy.
[15] Fan H., Yang W., Wang B., Yan Y., Fu Q., Fang D., Zhuang Z. ,2006, Design and manufacturing of a composite lattice structure reinforced by continuous carbon fibers, *Tsinghua Science and Technology* **11**(5): 515-522.
[16] Akbari Alashti R., Latifi Rostami S. A., Rahimi G. H., 2013, Buckling analysis of composite lattice cylindrical shells with ribs defects, *IJE Transactions A: Basics* **26**(4): 411-420.
[17] Ghorbanpour Arani A., Moslemian R., Arefmanesh A., 2009, Compressive behavior of glass/epoxy composite laminates with single delimitation, *Journal of Solid Mechanics* **1**:84-90.
[18] Jam J. E., Kia S. M., Ghorbanpour Arani A., Emdadi M., 2011, Elastic buckling of circular annular plate reinforced with carbon nanotubes, *Polymer Composites* **32**: 896-903.
[19] Qatu M. S., 2004, *Vibration of Laminated Shells and Plates*, First Edition, Elsevier Science Ltd.
[20] Hou A., 1997, *Strength of Composite Lattice Structures*, Ph.D Thesis, Georgia Institute of Technology.
[21] Hou A., Gramoll K., 1998, Compressive strength of composite lattice structures, *Journal of Reinforced Plastics and Composites* **17**: 462-483.
[22] Leissa A. W., 1973, *Vibration of Shells*, National Aeronautics and Space Administration , NASA, Washington, United States, NASA SP-288.
[23] Ansys Release 11.0 Inc, Company.
[24] Jones R. M., 1999, *Mechanics of Composite Materials*, *Material and Sciences Series*, Taylor & Francis Inc.